Movement Enhancement toward Multi-Scale Video Feature Representation for Temporal Action Detection

Zixuan Zhao Dongqi Wang Xu Zhao*
Department of Automation, Shanghai Jiao Tong University, China
{zhaozixuan, wangdq0124, zhaoxu}@sjtu.edu.cn

Abstract

Boundary localization is a challenging problem in Temporal Action Detection (TAD), in which there are two main issues. First, the submergence of movement feature, i.e. the movement information in a snippet is covered by the scene information. Second, the scale of action, that is, the proportion of action segments in the entire video, is considerably variable. In this work, we first design a Movement Enhance Module (MEM) to highlight movement feature for better action location, and then, we propose a Scale Feature Pyramid Network (SFPN) to detect multi-scale actions in videos. For Movement Enhance Module, firstly, Movement Feature Extractor (MFE) is designed to get the movement feature. Secondly, we propose a Multi-Relation Enhance Module (MREM) to grasp valuable information correlation both locally and temporally. For Scale Feature Pyramid Network, we design a U-Shape Module to model different scale actions, moreover, we design the training and inference strategy of different scales, ensuring that each pyramid layer is only responsible for actions at a specific scale. These two innovations are integrated as the Movement Enhance Network (MENet), and extensive experiments conducted on two challenging benchmarks demonstrate its effectiveness. MENet outperforms other representative TAD methods on ActivityNet-1.3 and THUMOS-14.

1. Introduction

Temporal Action Detection (TAD) is a significant video understanding task, which aims to extract video segments with specific action labels from untrimmed long videos. It remains a challenging problem because action boundaries are difficult to determine precisely, which adversely affects the performance in most works.

Two critical issues stand in the way of detecting action boundaries robustly from untrimmed videos. The first issue, which could be called as movement feature submergence, exists in where either context but not movement itself dominate feature expression, or movement is small in pixel size.

*Corresponding author

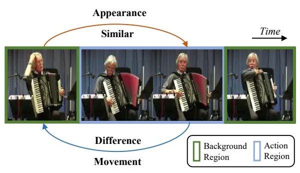

(a) Strong class-specific context.

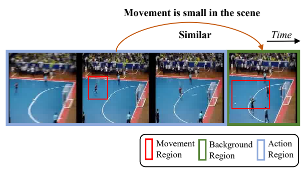

(b) Small movement in pixel size.

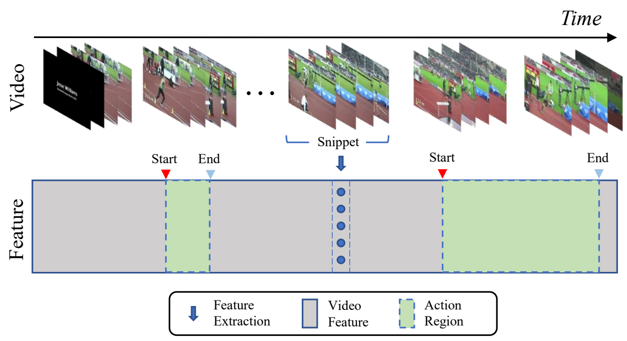

(c) Multi-scale actions.

Figure 1. Movement feature submergence and multi-scale actions. (a) Strong class-specific context of the *accordion* leads to video feature generated by TAC lacking the difference between action and background. (b) Small movement of *Futsal* results in less difference between action area and background area. (c) Multi-scale actions have different feature richness and action pattern.

For the first case, as shown in Fig 1(a), the action of Playing Accordion can be easily judged by *Accordion*, while this strong class-specific context causes the real movement information in action area to be submerged. For the second case, as shown in Fig 1(b), for Futsal, the stadium scene takes up a large proportion of pixels in the frame, while the movement information is ignored. This movement feature submergence leads to the feature in background to be similar with the feature in action area, which blues the action boundaries. If the movement information can be highlighted, the boundary will be easier to be located. However, this problem has been ignored by prior works [12, 29, 22].

The second issue is the multi-scale of actions in an untrimmed video. As shown in Fig 1(c), the feature richness varies greatly with the scale. There are rare features for action segments that account for a small proportion of the entire video, that is the small-scale action, and abundant features for those segments that account for a higher proportion, that is the large-scale action. We contend that there are different action patterns between different scales. Specifically, compared with small-scale action, large-scale action contains more obviously action process (*i.e.* start phase, action phase and end phase). Some researches [13, 7, 11] resort feature pyramid network (FPN) to solve the problem. However, there are two aspects that are ignored. Firstly, these works detect actions at different feature scales, but, they do not adaptively learn action features of different scales. Secondly, the information flow in FPN is insufficient, lacking interactions between different pyramid layers.

In this paper, as an effort to overcome the above challenges, we investigate the feature of TAD. (1) In order to overcome the movement feature submergence, and highlight the difference between foreground and background snippets. We design the Movement Enhance Module (MEM) to enhance the movement information in a video snippet, which includes two crucial parts. First, we propose a siamese network named Movement Feature Extractor (MFE), which uses the dynamic information of the frame sequence and the static information of the frame to extract movement feature from video snippets. And then, we propose the Multi-Relation Enhance Module (MREM) to establish temporal and local correlations between video snippets. (2) In order to learn specific representations for different scale actions, we propose the Scale FPN (SFPN), which uses a U-shaped network to produce multi-scale video features and facilitate the information flow between different layers. Moreover, for each layer in SFPN to take charge of detecting action segments of the corresponding scale, we design a two-stage learning strategy. In the former Generalization stage, each layer is trained with all action segments; in the latter Specialization stage, each layer is biased toward actions in a specific scale range. During inference, every layer takes charge of detecting action segments of the corresponding scale.

In summary, this work explores feature representation and action segment representation that are more suitable for TAD task. Its contributions are summarized as follows.

1. To alleviate the movement feature submergence, we design the Movement Enhance Module (MEM) to highlight the movement feature in a video snippet, and explore local and temporal relations between snippets.

2. For the multi-scale actions in an untrimmed video with different feature patterns, we design the Scale FPN (SFPN) to learn different scale actions respectively, where targeted training and inference strategies are adopted. Consequently, each layer in the SFPN specializes in actions at a certain scale range.

3. Extensive experiments conducted on two datasets verify the effectiveness of our proposed method. On ActivityNet1.3, MENet promotes the best average mAP from 36.6% to 37.7%, and boosts the mAP@0.7 from 31.8% to 34.0% on THUMOS-14.

2. Related Work

Video Feature for TAD. The pre-trained TAC model is often used as the feature extractor for Temporal Action Detection which receives several frames as a snippet to distill both appearance and motion information from raw video frames. TSN [26], I3D [3], and SlowFast [6] are the most common feature extractors. However, they only focus on the action categories, which results in some actions that are strongly related to the scene having quite similar representations to background segments. To overcome the drawback, TSP [1] adds additional background supervision in the pretraining model to generate the background-sensitive feature. BSP [28] artificially synthesizes different video boundaries and conducts boundary learning in the pretraining model to generate boundary-sensitive feature. However, these works cannot address the problem of movement feature submergence fundamentally. In this paper, MENet uses the Movement Enhance Module (MEM) to magnify the movement feature and the difference between action and background.

Multi-scale Action Detection. The scale of the action varies dramatically in a video. Compared with the large actions, those small action segments have fewer samples and insufficient features. Some works [13, 7, 11] focus on feature pyramid network (FPN) to generate different temporal resolution features. However, the FPN structure does not learn specific feature representation for a certain action scale, and also lacks sufficient information flow intrinsically. TSI [15] proposes a scale-invariant loss, which balances large and small actions in quantity, but fails to fundamentally solve the scarce feature of small actions. In this work, we propose SFPN to cope with these problems, which establishes associations between different scale features and learns scale-specific feature representations.

Temporal Action Detection. Benefiting from the successful practice of image object detection and trimmed video action recognition, the two-stage pipeline prevails in TAD task. Specifically, the first stage is to locate candidate action segments in the video, and the second stage uses an action classifier to classify these proposals. The first stage has three main paradigms. (1) Anchor-Based method: Methods [5, 13, 21] put anchors of various scales on the video feature, and then give the final confidence of anchors. However, they cannot produce flexible boundaries. (2) Boundary-Base method: Methods [14, 31, 16] predict boundary scores on the video feature, which are combined to generate proposals. However, the confidence of the proposal lacks global information. (3) Combined method: Methods [12, 10, 4] combine these two methods to generate precise confidence and flexible boundaries. In this work, we follow the combined method to integrate the start point and end point as a proposal and generate multi-scale anchor maps to predict anchor confidence.

3. Method

3.1. Overview

Problem Definition. Input of the Movement Enhance Network (MENet) is an untrimmed video denoted as $V = \{v_i\}_{i=1}^{L_v}$, where v_i represents the i-th frame of the video and L_v is the total frames. The duration of the video is T_v. Due to redundancy between video frames, several consecutive frames are usually regarded as a snippet. With the sampling interval σ, the whole video can be defined as snippet sequence $S = \{s_i\}_{i=1}^{L_s}$, $L_s = L_v/\sigma$ representing the number of total snippets. The output of the MENet is $\{\psi_i|\psi_i = (t_{i,s}, t_{i,e}, c_i, score_i)\}$ where $t_{i,s}, t_{i,e}, c_i$ and $score_i$ are start time, end time, action category and confidence score, respectively. The annotations of untrimmed video are action instances $\{\Psi_i|\Psi_i = (t^*_{i,s}, t^*_{i,e}, c^*_i)\}$.

Framework Architecture. The framework architecture of MENet is shown in Fig 2. MENet is mainly composed of two parts: Movement Enhance Module (MEM) and Scale FPN (SFPN). MEM is used to extract movement enhanced feature and explore different video relations between snippets. SFPN is proposed to generate feature pyramid and learn specific expression patterns of different action scales. Finally, SFPN gives action boundaries and confidence scores of different scale actions, separately.

3.2. Movement Enhance Module

To obtain the feature that contains action category information and is sensitive to foreground and background, simultaneously, we propose the Movement Enhance Module, which contains two vital stages: Movement Feature Extractor (MFE) and Multi-Relation Enhance Module (MREM).

Movement Feature Extractor. In order to amplify the movement information, MFE is proposed. As shown in Fig 3, MFE uses a siamese network to highlight the movement information in a video snippet. We select R(2+1)D-34 [24] as backbone with the TAC pretrained weight on Kinetics-400 [9], and two networks share the weight. MFE has two input paths. One path is video snippet path composed of consecutive frames, and the other is frame duplication path, which selects a frame from the snippet and copies it to the length of the snippet. Here, the middle frame is selected for duplication. The feature from the video snippet path contains both static scene and dynamic movement information, which is $F_{Total} \in \mathbb{R}^{C' \times T}$, but feature from the frame duplication path only contains static scene information, which is $F_{Static} \in \mathbb{R}^{C' \times T}$. And then, MFE extracts the movement information in the snippet using the difference between the two features, which is defined as $F_{Movement} \in \mathbb{R}^{C' \times T}$. Finally, $F_{Movement}$ and F_{Total} are concatenated as $F_{MT} \in \mathbb{R}^{2C' \times T}$.

Multi-Relation Enhance Module. To establish relations between snippets and fuse the information at semantic dimension, the Multi-Relation Enhance Module is proposed. As shown in Fig 2, firstly, we use a 1D convolution to fuse information at semantic dimension. Secondly, there are three information paths in MREM. (1) Local Path: 1D convolution can directly establish relations in a local scale k, where k is the kernel size. However, it is difficult for 1D convolutions to establish temporal relationship between snippet features. (2) Forward Path: The LSTM processes each snippet successively according to the input order, with an outstanding ability to model the temporal relation. In forward path, we use LSTM to establish forward information. (3) Backward Path: In backward path, we flip the video sequence, and establish backward information. Finally, the three paths are integrated.

3.3. Scale Feature Pyramid Network

We contend different scale actions have different patterns. Therefor, the SFPN is designed to learn patterns of specific scales. SFPN contains U-Shape Module and Detector Head, which aims to generate feature pyramid and final detection results, respectively.

U-Shape Module. For feature pyramid generating, as shown in Fig 2, SFPN uses a U-shaped architecture inspired by [20] to generate feature sequences in different temporal resolution. From top to down, SFPN uses multiple temporal convolution layers followed by AvgPooling to downsample the temporal resolution. From bottom to up, to restore the lower layer information, SFPN uses several 1D transpose convolution to restore the feature resolution and features in the same resolution are concatenated.

Detector Head. As demonstrated in Fig 2, each detector head consists of a Boundary Predictor, an Anchor Feature Align Layer and two Anchor Score Predictor (ASP). The output of the Boundary Predictor and Anchor Score Predictor is used to generate proposals and confidence scores, and the Anchor Feature Align Layer is to generate the feature representation for each anchor.

Boundary Predictor. Boundary Predictor aims at predicting boundary probabilities $P_s = \{p_s^i\}_{i=1}^{L_i}, P_e = \{p_e^i\}_{i=1}^{L_i}$ of each snippet by recognizing the boundary pattern.

Anchor Feature Align Layer. The area between any two snippets can form an anchor, and each anchor consists of several consecutive snippets. Supposing N_i anchors are randomly sampled to participate in the forward. The Anchor Feature Align Layer adopts SGAlign designed in [29]

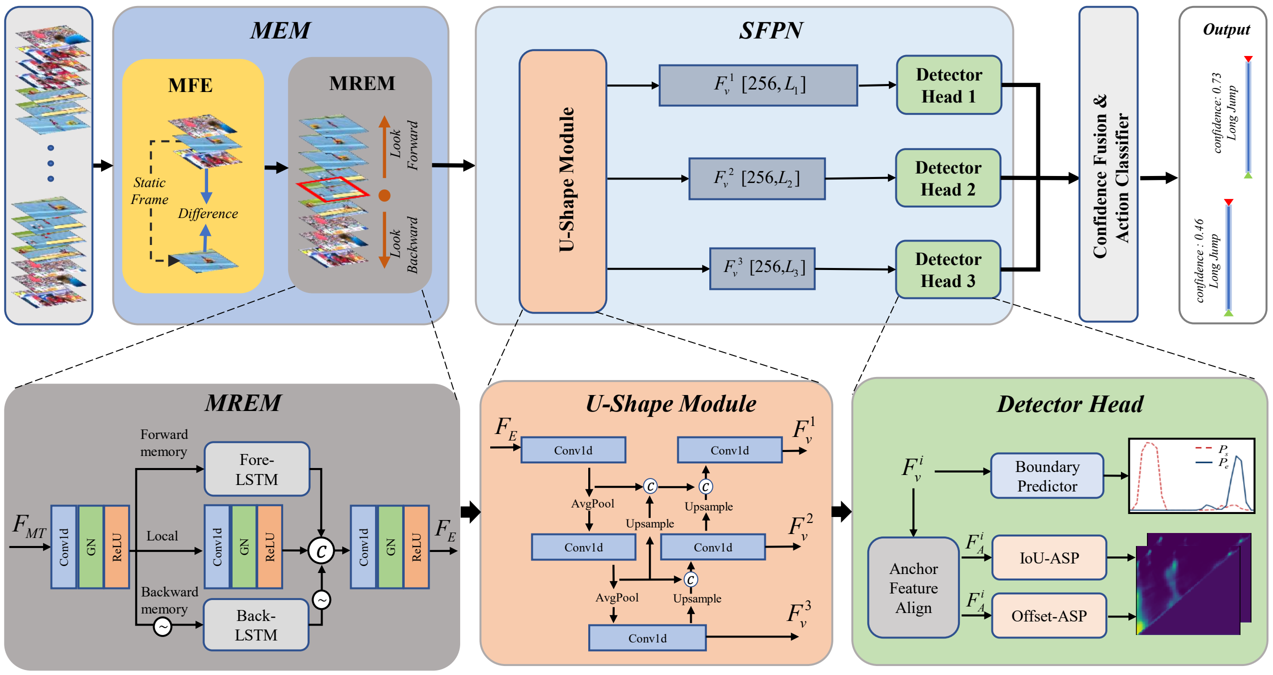

Figure 2. Overview of our MENet and the structure of some sub-modules. There are two crucial parts in the framework (*Top*) of MENet: Movement Enhance Module (MEM) and Scale FPN (SFPN). MEM is designed to generate movement enhanced feature. SFPN is designed to generate multi-scale feature pyramid, and learn action expressions in different layers. The structure of the sub-modules is shown below (*Bottom*) with the same color in the framework.

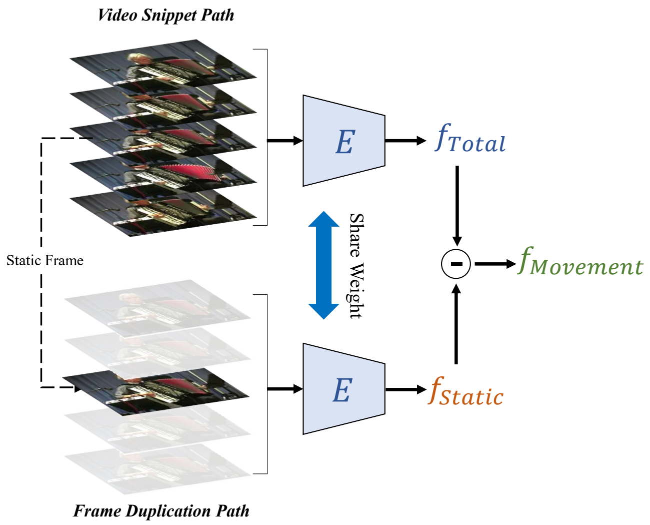

Figure 3. Illustration of MFE. This module constructs the movement feature in a snippet by the difference between dynamic video snippet and static picture.

to generate feature expressions $F_A^i \in \mathbb{R}^{C \times S \times N_i}$ for anchors from the video feature F_v^i, where S is the sampling number of snippets within an anchor.

Anchor Score Predictor. IoU-ASP and Offset-ASP have the same structure to recognize the action pattern within an anchor. For the i-th layer in SFPN, IoU-ASP generates two maps $M_{cls}^i \in \mathbb{R}^{D_i \times L_i}$, $M_{reg}^i \in \mathbb{R}^{D_i \times L_i}$, where D_i is predefined maximum anchor duration. In Offset-ASP, two output maps are denoted as$M_{cent}^i \in \mathbb{R}^{D_i \times L_i}$, $M_{dura}^i \in \mathbb{R}^{D_i \times L_i}$. These two maps indicate each anchor's center offset and duration offset respectively.

3.4. Specific action pattern Learning

Actions of different scales have different feature representations. Correspondingly, different layers in SFPN have different feature granularity and temporal resolution. Therefore, we advocate applying a targeted training strategy for actions at different scales, assuring that each layer in SFPN is only responsible for actions at a specific scale range. Specifically, define the scale $S \in [0, 1]$ as the ratio of action length to video length. Then the first layer (the top layer of the pyramid) with the longest sequence is responsible for small-scale actions whose scale in $[S_{min}^1, S_{max}^1]$, and the second layer (the middle layer of the pyramid) with a moderate sequence length is responsible for medium-scale actions whose scale in $[S_{min}^2, S_{max}^2]$. The remaining third layer with the shortest sequence is responsible for large-scale actions whose scale belongs to $[S_{min}^3, S_{max}^3]$. To implement this idea, a two-stage training strategy is designed.

Two-stage training strategy. The two-stages of training ASP are Generalization and Specialization, respectively. Due to the different lengths of feature sequences, the to-

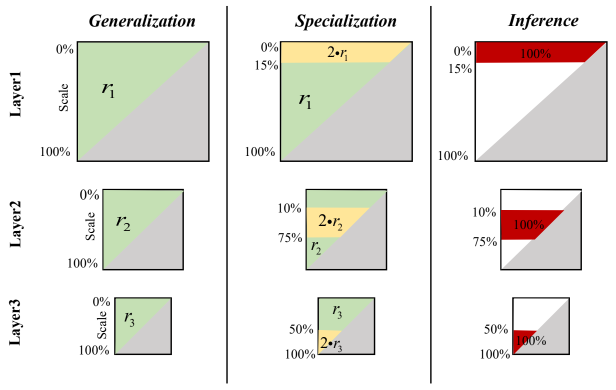

Figure 4. The two-stage training strategy (left column and middle column) and the inference strategy (right column) of ASP. Each square represents an anchor map of a layer, the grey area is the invalid region. Other colors represent different sampling ratios in a certain scale range, with white, green, yellow and red representing 0%, r_i, $2r_i$ and 100% respectively.

tal number of dense anchors contained in each layer varies. In order to ensure that each layer is trained equally and reduce the computational cost, different anchor sampling ratios r_1, r_2, r_3 are set for the three layers, where $0\% < r_1 \leq r_2 \leq r_3 \leq 100\%$. (1) In the former Generalization stage, given the sampling ratio r_i, randomly sample $N_i = \binom{L_i}{2} \cdot r_i$ anchors from valid region to train the IoU-ASP and Offset-ASP of i-th layer, as shown in the left column of Fig 4. The purpose of this stage is to let ASP learn a general pattern of all actions. (2) In the latter Specialization stage, for the i-th layer in SFPN, the training samples come from two parts, as shown in the middle column in Fig 4. The first part are randomly sampled according to the sampling rate of $min(100\%, 2 \cdot r_i)$ from anchors whose scale in $[S^i_{min}, S^i_{max}]$ (yellow area in Fig 4). The second part are sampled from the remaining anchors whose scale in $(0, S^i_{min})$ or $(S^i_{max}, 100\%]$, with the sampling rate of r_i (green area in Fig 4). This Specialization stage highlights the effect of anchors at the certain scale range, making the detection head of each layer more specialized.

3.5. Training & Inference

Label Assignment. Assuming the video duration is L_v, each snippet corresponds to a video period. In annotation, a ground-truth action which starts at t^*_s and ends at t^*_e. Expanding boundary from moment to region, the start region is defined as $R_s = [t^*_s - 1.5\frac{T_v}{L_i}, t^*_s + 1.5\frac{T_v}{L_i}]$ and end region is defined as $R_e = [t^*_e - 1.5\frac{T_v}{L_i}, t^*_e + 1.5\frac{T_v}{L_i}]$. For Boundary Predictor, compute the overlap between each snippet period and R_s as the label of start probabilities $G^i_s \in \mathbb{R}^{L_i}$. Similarly, compute the overlap between snippet period and R_e as the label of end probabilities G^i_e. For IoU-ASP, following [12], tIoU between each anchor and all actions are calculated and then arranged into a map $G^i_{IoU} \in \mathbb{R}^{D_i \times L_i}$. Anchors with tIoU score greater than 0.9 participate in the training of Offset-ASP. For anchor start at t_s and end at t_e, assuming its corresponding ground-truth action is $[t^*_s, t^*_e]$, the center offset Δc and duration offset Δd are calculated as Eq. (1)- (2), and arranged into maps $G^i_{cent} \in \mathbb{R}^{D_i \times L_i}$ and $G^i_{dura} \in \mathbb{R}^{D_i \times L_i}$.

$$c = \frac{t_s + t_e}{2}, d = t_e - t_s, c^* = \frac{t^*_s + t^*_e}{2}, d^* = t^*_e - t^*_s \tag{1}$$

$$\Delta c = \frac{c^* - c}{d}, \Delta d = \log\frac{d^*}{d} \tag{2}$$

Basic Loss. (1) For the i-th layer, the loss of Boundary-Predictor is the re-weighted binary cross-entropy loss L_B Eq. 3, where $P = \{p_t\}^{L_i}_{t=1}$ and $G = \{g_t\}^{L_i}_{t=1}$ represent the predicted boundary probabilities and its label of all snippets, respectively. Snippets with $g_t > 0.5$ serve as positive samples (*i.e.*, $\delta\{g_t > 0.5\} = 1$) and others are negative samples. T^+_i and T^-_i are the number of positive and negative samples in this layer respectively. (2) The loss of IoU-ASP is the re-weighted binary cross-entropy loss L_{asp} Eq. 4 and L2 loss L_2, where $M = \{m_j\}^{N_i}_{j=1}$ and $G = \{g_j\}^{N_i}_{j=1}$ represent the predicted value and ground-truth value of each sampled anchor in the i-th layer. N_i, N^+_i, N^-_i represent the number of sampled anchors, positive anchors whose tIoU greater than 0.9 and negative anchors of this layer, respectively. (3) The loss of Offset-ASP is Smooth L1 loss L_1. Note that only those sampled anchors with tIoU greater than 0.9 participate in the training of Offset-ASP. The re-weights in L_B and L_{asp} are used to balance the number between positive and negative samples.

$$\begin{aligned} L_B(P,G) = -\frac{1}{L_i}\sum^{L_i}_{t=1}(\frac{L_i}{T^+_i} \cdot \delta\{g_t > 0.5\} \cdot \log p_t \\ + \frac{L_i}{T^-_i}(1 - \delta\{g_t > 0.5\} \cdot \log(1 - p_t)) \end{aligned} \tag{3}$$

$$\begin{aligned} L_{asp}(M,G) = -\frac{1}{N_i}\sum^{N_i}_{j=1}(\frac{N_i}{N^+_i} \cdot \delta\{g_j > 0.9\} \cdot \log m_j \\ + \frac{N_i}{N^-_i}(1 - \delta\{g_j > 0.9\} \cdot \log(1 - m_j)) \end{aligned} \tag{4}$$

Total Loss. The loss of the i-th layer is composed of three parts: boundary loss, IoU loss and offset loss, as shown in Eq.(5) (6) (7) respectively. The total training objective is the sum of all three layers, formulated as Eq. 8. Besides, in order to balance the value between different terms, the coefficient $\lambda 1$ and $\lambda 2$ are set as 5 and 10.

$$L^i_{bound} = L_B(P^i_s, G^i_s) + L_B(P^i_e, G^i_e) \tag{5}$$

$$L^i_{IoU} = L_{asp}(M^i_{cls}, G^i_{IoU}) + \lambda_1 \cdot L_2(M^i_{reg}, G^i_{IoU}) \tag{6}$$

$$L^i_{off} = L_1(M^i_{cent}, G^i_{cent}) + L_1(M^i_{dura}, G^i_{dura}) \tag{7}$$

$$L_{total} = \sum_{i=1}^{3}(L_B^i + L_{IoU}^i + \lambda_2 \cdot L_{off}^i) \tag{8}$$

Inference. Each layer outputs P_s^i, P_e^i, M_{cls}^i, M_{reg}^i, M_{cent}^i and M_{dura}^i from the detector head in inference. Following [14, 12, 15], snippet in boundary probability P_s is screened out as candidate start point if it is local peak or its probability is greater than $0.5 \cdot \max(P_s)$. And snippets can be selected as candidate end point from P_e in the same way. Then the candidate start and end points are combined into proposals. In order to produce the more reasonable proposals, as shown in Fig 4, each layer of SFPN only outputs anchors in the corresponding scale range. Specifically, for the i-th layer, its responsible scale range is $[S_{min}^i, S_{max}^i]$. Furthermore, in the proposals set, for any start snippet whose index is sdx and centered at time t_1, and the end snippet whose index is edx and centered at time t_2, we can get its start probability $p_s = P_s^i[sdx]$, end probability $p_e = P_e^i[edx]$ and tIoU score $p_{IoU} = M_{cls}^i[edx-sdx, sdx] \cdot M_{reg}^i[edx-sdx, sdx]$. Its center is $c = (sdx + edx)/2L_i$ and duration is $d = (edx - sdx)/L_i$. Subsequently, to refine the boundary, we can obtain center offset $\Delta c = M_{cent}^i[edx - sdx, sdx]$ and duration offset $\Delta d = M_{dura}^i[edx - sdx, sdx]$, and adjust the boundary to (t_1', t_2') as Eq. 9:

$$\begin{aligned} c' &= d \cdot \Delta c + c, d' = d \cdot e^{\Delta d} \\ t_1' &= c' - \frac{d'}{2}, t_2' = c' + \frac{d'}{2} \end{aligned} \tag{9}$$

Finally, proposals generated by each layer are merged together, and the action classifier assigns every proposal with a certain label and a classification score P_{label}. The final score for the proposal (t_1', t_2') is shown as Eq. 10. Then Soft-NMS [32] is adopted to remove redundant segments.

$$score_{t_1', t_2'} = p_s \cdot p_e \cdot p_{IoU} \cdot p_{label} \tag{10}$$

4. Experiments

4.1. Dataset and Settings

Dataset. In order to verify the effectiveness of MENet, we experiment on two challenging datasets. **ActivityNet-1.3** [2] contains 200 categories of daily life, sports, *etc*. We use the training set for model training and report the performance on the validation set. **THUMOS-14** [8] consists of 413 videos with 20 action classes which is almost sports. In THUMOS-14, the validation set contains 200 long videos, including 3007 action segments, and the test set contains 213 videos, including 3358 action segments. Following the standard practice of THUMOS-14, we train MENet on the validation set and valid it on the test set.

Metric. In order to fully demonstrate the advantages of our proposed method, we use two main evaluation metrics: mAP under a certain temporal tIoU threshold (mAP@tIoU) and average recall at a specified average number of proposals (AR@AN). Besides, on ActivityNet, the area under the AR-AN curve (AUC) also serves as a metric.

Network Details. We use R(2+1)D-34 as backbone with the TAC pretrained weight on Kinetics-400 serving as the primary feature extractor. The sampling interval σ set as 16 frames and 5 frames for ActivityNet-1.3 and THUMOS-14, respectively. In this way, for the input video with L_v frames, video snippet length $L_s = L_v/\sigma$. For ActivityNet-1.3, we use linear interpolation to resize the length of video features $T = 200$. For a long video in THUMOS-14, a sliding window with a length of 256 and an overlap of 50% is used to truncate the original video feature. Each window is detected independently, and finally the results of all windows are concatenated as the total result of the entire long video. The scale ranges of each layer in the pyramid are set as: $[S_{min}^1, S_{max}^1] = [0, 15\%]$, $[S_{min}^2, S_{max}^2] = [10\%, 75\%]$ and $[S_{min}^3, S_{max}^3] = [50\%, 100\%]$. As for the action classifier, following the routine of most two-stage TAD methods, Untrimmed Net [25] serves as the classifier for THUMOS-14, and the recognition model by [32] for ActivityNet-1.3.

Implementation Details. MENet is trained by Adam algorithm with batch size 8 and learning rate 10^{-3}. The sampling ratio of each layer r_1, r_2, r_3 are set as 50%, 40%, 90%, respectively. For ActivityNet-1.3, the training process takes 10 epochs, where the first 7 epochs is the Generalization stage and the rest is the Specialization stage. As for THUMOS-14, the total training epoch is 7, and only the first epoch is the Generalization stage. Besides, the learning rate is decayed to 10^{-4} after 5 epochs on THUMOS-14 and 7 epochs on ActivityNet-1.3.

4.2. Performance Evaluation On Detection

We compare MENet with other state-of-the-art methods on ActivityNet-1.3 and THUMOS-14. Table 1 shows the comparison on the validation set of ActivityNet-1.3. The mAP at tIoU thresholds of $\{0.5, 0.75, 0.95\}$ are reported, as well as the Avg.mAP which is calculated at tIoU thresholds between 0.5 and 0.95 with the step of 0.05. Impressively, MENet outperforms other representative methods at tIoU thresholds 0.75 and 0.95. MENet promotes the Avg.mAP from 36.6% to 37.7%, with an increase of more than 1.1%. Comparing the methods of different backbones, MENet exceeds others.

Table 2 presents the detection performance comparison on the test set of THUMOS-14. MENet achieves comparable performance with the best method [30] at low tIoU thresholds. But, MENet outperforms other representative methods at tIoU thresholds 0.6 and 0.7. MENet improves the mAP@0.7 from the current best 31.8% to 34.0%. To locate the boundaries more accurately, a higher threshold is usually used to separate the positive and negative samples in training. Therefore MENet has a better response at high tIoU thresholds. Higher tIoU means more precise action boundaries, which is more difficult and more important for action localization. Meanwhile, it is noteworthy that MENet shows obvious superiority compared with other FPN-based methods like [11], which substantiates the effectiveness of the SFPN proposed in MENet.

Method	Backbone	mAP@tIoU (%)			
		0.5	0.75	0.95	Avg.
GTAN [16]	P3D	52.6	34.1	8.9	34.3
BSN [14]	TSN	46.5	30.0	8.0	30.0
BMN [12]	TSN	50.1	34.8	8.3	33.9
G-TAD [29]	TSN	50.4	34.6	9.0	34.1
PCMNet [18]	TSN	51.4	36.1	9.5	35.3
TCA-Net [19]	TSN	52.3	36.7	6.9	35.5
RTD-Net [23]	I3D	47.2	30.7	8.6	30.8
ContextLoc [33]	I3D	56.0	35.2	3.6	34.2
AFSD [11]	I3D	52.4	35.3	6.5	34.4
TAGS [17]	I3D	**56.3**	36.8	9.6	36.5
STPT [27]	STPT	51.4	33.7	6.8	33.4
ActionFormer [30]	R(2+1)D	54.7	37.8	8.4	36.6
MENet(ours)	R(2+1)D	54.7	**38.4**	**10.5**	**37.7**

Table 1. The temporal action detection performance comparison with state-of-art methods on ActivityNet-1.3. Bold text indicates the best results.

Method	Backbone	mAP@tIoU (%)				
		0.3	0.4	0.5	0.6	0.7
GTAN [16]	P3D	57.8	47.2	38.8	-	-
BSN [14]	TSN	53.5	45.0	36.9	28.4	20.0
BMN [12]	TSN	56.0	47.4	38.8	29.7	20.5
G-TAD [12]	TSN	54.5	47.6	40.2	30.8	23.4
PCMNet [18]	TSN	61.5	55.4	47.2	37.5	27.3
TCA-Net [19]	TSN	60.6	53.2	44.6	36.8	26.7
RTD-Net [23]	I3D	68.3	62.3	51.9	38.8	23.7
ContextLoc [33]	I3D	68.3	63.8	54.3	41.8	26.2
AFSD [11]	I3D	67.3	62.4	55.5	43.7	31.1
TAGS [17]	I3D	68.6	63.8	57.0	46.3	31.8
STPT [27]	STPT	70.6	65.7	56.4	44.6	30.5
ActionFormer [30]	R(2+1)D	**73.4**	**67.4**	**59.1**	46.7	31.5
MENet(ours)	R(2+1)D	70.7	65.3	58.8	**49.1**	**34.0**

Table 2. The temporal action detection performance comparison with state-of-art methods on THUMOS-14. Bold text indicates the best results.

4.3. Performance Evaluation On Proposal

To further verify the advantages of MENet, we do not consider action classes of action segments to evaluate its performance on temporal action proposal (TAP) task.

Through Table 3, we can further discover the performance improvement of AR@100 and the area under the AR-AN curve (AUC) on ActivityNet-1.3. For instance, MENet boosts the AUC from 68.1% to 70.2%. As for THUMOS-14, MENet outperforms other methods in all metrics are reported in Table 4, which certifies the effectiveness of MENet once again.

4.4. Ablation Study

Ablation studies are performed thoroughly to verify the role of each module in MENet, as well as the impact of different training strategies.

Method	AR@100	AUC
BSN [14]	74.2	66.2
GTAN [16]	74.8	67.1
BMN [12]	75.0	67.1
RTD-Net [23]	73.2	65.8
TCA-Net [19]	76.1	68.1
MENet(ours)	**77.0**	**70.2**

Table 3. Temporal action proposal performance comparison with other representative methods on ActivityNet-1.3. Bold text indicates the best results.

Method	AR@50	AR@100	AR@200	AR@500
BSN [14]	37.5	46.1	53.2	60.6
BMN [12]	39.4	47.7	54.7	62.1
RTD-Net [23]	41.5	49.32	56.41	62.91
TCA-Net [19]	42.1	50.5	57.1	63.6
MENet(ours)	**44.2**	**52.3**	**58.6**	**66.0**

Table 4. Temporal action proposal performance comparison with other representative methods on THUMOS-14, measured by AR@AN. Bold text indicates the best results.

1). ***Effectiveness of the MEM***: As discussed before, when constructing the movement enhance feature, MFE and MREM are the crucial designs in MEM. To certify the function of these two modules, we design a Base model for comparison, in which the Movement Feature is removed and MREM is replaced by temporal 1D convolution. As shown in Table 5, we can find that compared with the Base model, Movement Feature and MREM both can promote the performance. Besides, the best results emerge when combining them together as the intact MEM.

Construction	mAP@tIoU (%)			
	0.5	0.75	0.95	Avg.
Base	54.2	37.3	10.4	37.0
Base + Movement Feature	54.5	37.8	10.6	37.3
Base + MREM	54.4	37.9	10.4	37.3
MEM	54.7	38.4	10.5	**37.7**

Table 5. Ablation study on the MEM. The Detection performance is reported on ActivityNet-1.3. And The best result can be achieved with these two modules are integrated.

2). ***Effectiveness of the U-shape Module***: As discussed before, when constructing the feature pyramid, U-shape Module is designed to establish interactions between different layers. To reveal the validity of this idea, we use 1D convolution with the step of 2 and AvgPooling to downsample the feature sequence respectively. From Table 6, the U-shape Module can promote the performance, which substantiates the importance of this design.

3). ***Effectiveness of feature pyramid structure***: For better detection accuracy, MENet makes use of the feature pyramid. To verify the impact of this structure, we only use a single layer feature sequence to conduct experiments

Construction	mAP@tIoU (%)			
	0.5	0.75	0.95	Avg.
DownSampling (AvgPooling)	54.5	38.2	10.2	37.4
DownSampling (Convolution)	54.4	38.1	10.8	37.3
U-shape Module	54.7	38.4	10.5	**37.7**

Table 6. Ablation study on the U-shape Module. The Detection performance is reported on ActivityNet-1.3.

and compare it with the SFPN, keeping other components unchanged. On ActivityNet-1.3, single-layer feature with lengths of 200, 100 and 50 are used. Corresponding results are shown in Table 7. The experimental results exhibit that SFPN performs better than any other single-layer structure, thus justifying the feature pyramid structure is indeed beneficial to the performance.

Length	mAP@tIoU (%)			
	0.5	0.75	0.95	Avg.
50	53.0	37.1	10.8	36.8
100	54.1	38.1	10.4	37.1
200	54.2	38.3	10.5	37.3
SFPN	54.7	38.4	10.5	**37.7**

Table 7. Ablation study on the SFPN. "Length" means the temporal length of single layer feature sequence. The Detection performance is reported on ActivityNet-1.3.

4). ***Effectiveness of two-stage training***: For efficient training of MENet and ensuring that the i-th layer in SFPN is specialized in actions at a specific scale range $[S^i_{min}, S^i_{max}]$, the two-stage training strategy is applied. When training ASP of the i-th layer, in the first Generalization stage, the anchors are randomly selected from all scales according to the sampling ratio r_i, in the second Specialization stage, the sampling ratio inside and outside the range $[S^i_{min}, S^i_{max}]$ are $2 \cdot r_i$ and r_i, respectively. In this ablation study, we train MENet using the fully Generalization stage, the fully Specialization stage and the complete two-stage strategy, respectively. In addition, to demonstrate the effectiveness of this training method, we also test a new Bias training strategy that only samples from the range $[S^i_{min}, S^i_{max}]$ with the sampling ratio of r_i.

As shown in Table 8, the performance of the Bias strategy is the worst, indicating that in addition to those samples in the specific scale range, other samples outside this range also play an important role for a better understanding of actions. Further, the training effect is impeded when removing either the Generalization or the Specialization stage, which verifies the effectiveness of the two-stage training strategy.

5). ***Qualitative Comparison***: To illustrate the edge of MENet more intuitively, we select videos of Javelin Throw and High Jump from ActivityNet-1.3 and compare our results qualitatively with the Base, in which we remove the movement enhanced feature and SFPN. Results with the

Training Strategy	mAP@tIoU (%)			
	0.5	0.75	0.95	Avg.
only Bias	45.8	29.1	7.4	29.4
only Generalization	54.3	38.2	11.0	37.4
only Specialization	54.6	38.0	10.8	37.4
two-stage	54.7	38.4	10.5	**37.7**

Table 8. Ablation study on the two-stage training strategy. The proposed two-stage training leads to better performance than the single stage method or the Bias method.

highest confidence score are visualized in Fig 5. Firstly, Compared with the Base method, MENet uses the movement feature, which enlarges the difference between action and background, making the model more accurate in boundary localization. Secondly, it can be seen the High Jump action contains a large-scale action and a small-scale action. Due to the SFPN in MENet, MENet can better capture actions at different scales. Results of qualitative comparison once again prove the superiority of MENet.

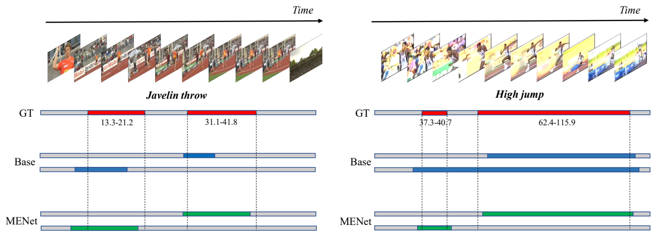

Figure 5. Qualitative Comparison. MENet generates more accurate action segments.

5. Conclusion

Temporal action detection (TAD) is aimed at localizing the action segment and classifying the action class. Despite the considerable attention and rapid development, TAD is hindered by two critical problems: the movement feature submergence and multi-scale action detection. In an effort to overcome these two challenges, we propose the Movement Enhance Network (MENet) with two crucial designs. Firstly, we propose the Movement Enhance Module (MEM) to extract the movement feature in video snippets and explore the multi-relations between the snippets. Secondly, we propose the Scale FPN (SFPN) to handle the different scale actions, we design the U-shape Module to facilitate the information flow between different scale features. For better performance, we design the training and inference stage, ensuring that each layer in MENet is specialized at a specific scale range. Extensive experiments demonstrate that MENet considerably outperforms other representative TAD methods on ActivityNet-1.3 and THUMOS-14.

Acknowledgements. This work was supported by National Natural Science Foundation of China (NSFC) No. 62176156.

References

[1] Humam Alwassel, Silvio Giancola, and Bernard Ghanem. Tsp: Temporally-sensitive pretraining of video encoders for localization tasks. In *ICCV*, pages 3173–3183, 2021.

[2] Fabian Caba Heilbron, Victor Escorcia, Bernard Ghanem, and Juan Carlos Niebles. Activitynet: A large-scale video benchmark for human activity understanding. In *CVPR*, pages 961–970, 2015.

[3] Joao Carreira and Andrew Zisserman. Quo vadis, action recognition? a new model and the kinetics dataset. In *CVPR*, pages 6299–6308, 2017.

[4] Guo Chen, Yin-Dong Zheng, Limin Wang, and Tong Lu. Dcan: Improving temporal action detection via dual context aggregation. In *AAAI*, volume 36, pages 248–257, 2022.

[5] Xiyang Dai, Bharat Singh, Guyue Zhang, Larry S Davis, and Yan Qiu Chen. Temporal context network for activity localization in videos. In *ICCV*, pages 5793–5802, 2017.

[6] Christoph Feichtenhofer, Haoqi Fan, Jitendra Malik, and Kaiming He. Slowfast networks for video recognition. In *ICCV*, pages 6202–6211, 2019.

[7] Yupan Huang, Qi Dai, and Yutong Lu. Decoupling localization and classification in single shot temporal action detection. In *ICME*, pages 1288–1293. IEEE, 2019.

[8] Yu-Gang Jiang, Jingen Liu, A Roshan Zamir, George Toderici, Ivan Laptev, Mubarak Shah, and Rahul Sukthankar. Thumos challenge: Action recognition with a large number of classes, 2014.

[9] Will Kay, Joao Carreira, Karen Simonyan, Brian Zhang, Chloe Hillier, Sudheendra Vijayanarasimhan, Fabio Viola, Tim Green, Trevor Back, Paul Natsev, et al. The kinetics human action video dataset. *arXiv preprint arXiv:1705.06950*, 2017.

[10] Chuming Lin, Jian Li, Yabiao Wang, Ying Tai, Donghao Luo, Zhipeng Cui, Chengjie Wang, Jilin Li, Feiyue Huang, and Rongrong Ji. Fast learning of temporal action proposal via dense boundary generator. In *AAAI*, volume 34, pages 11499–11506, 2020.

[11] Chuming Lin, Chengming Xu, Donghao Luo, Yabiao Wang, Ying Tai, Chengjie Wang, Jilin Li, Feiyue Huang, and Yanwei Fu. Learning salient boundary feature for anchor-free temporal action localization. In *CVPR*, pages 3320–3329, 2021.

[12] Tianwei Lin, Xiao Liu, Xin Li, Errui Ding, and Shilei Wen. Bmn: Boundary-matching network for temporal action proposal generation. In *ICCV*, pages 3889–3898, 2019.

[13] Tianwei Lin, Xu Zhao, and Zheng Shou. Single shot temporal action detection. In *ACMMM*, pages 988–996, 2017.

[14] Tianwei Lin, Xu Zhao, Haisheng Su, Chongjing Wang, and Ming Yang. Bsn: Boundary sensitive network for temporal action proposal generation. In *ECCV*, pages 3–19, 2018.

[15] Shuming Liu, Xu Zhao, Haisheng Su, and Zhilan Hu. Tsi: Temporal scale invariant network for action proposal generation. In *ACCV*, 2020.

[16] Fuchen Long, Ting Yao, Zhaofan Qiu, Xinmei Tian, Jiebo Luo, and Tao Mei. Gaussian temporal awareness networks for action localization. In *CVPR*, pages 344–353, 2019.

[17] Sauradip Nag, Xiatian Zhu, Yi-Zhe Song, and Tao Xiang. Proposal-free temporal action detection via global segmentation mask learning. In *ECCV*, pages 645–662, 2022.

[18] Xin Qin, Hanbin Zhao, Guangchen Lin, Hao Zeng, Songcen Xu, and Xi Li. Pcmnet: Position-sensitive context modeling network for temporal action localization. *Neurocomputing*, 510:48–58, 2022.

[19] Zhiwu Qing, Haisheng Su, Weihao Gan, Dongliang Wang, Wei Wu, Xiang Wang, Yu Qiao, Junjie Yan, Changxin Gao, and Nong Sang. Temporal context aggregation network for temporal action proposal refinement. In *CVPR*, pages 485–494, 2021.

[20] Olaf Ronneberger, Philipp Fischer, and Thomas Brox. U-net: Convolutional networks for biomedical image segmentation. In *MICCAI*, pages 234–241, 2015.

[21] Zheng Shou, Dongang Wang, and Shih-Fu Chang. Temporal action localization in untrimmed videos via multi-stage cnns. In *CVPR*, pages 1049–1058, 2016.

[22] Haisheng Su, Weihao Gan, Wei Wu, Yu Qiao, and Junjie Yan. Bsn++: Complementary boundary regressor with scale-balanced relation modeling for temporal action proposal generation. In *AAAI*, volume 35, pages 2602–2610, 2021.

[23] Jing Tan, Jiaqi Tang, Limin Wang, and Gangshan Wu. Relaxed transformer decoders for direct action proposal generation. In *ICCV*, pages 13526–13535, 2021.

[24] Du Tran, Heng Wang, Lorenzo Torresani, Jamie Ray, Yann LeCun, and Manohar Paluri. A closer look at spatiotemporal convolutions for action recognition. In *CVPR*, pages 6450–6459, 2018.

[25] Limin Wang, Yuanjun Xiong, Dahua Lin, and Luc Van Gool. Untrimmednets for weakly supervised action recognition and detection. In *CVPR*, pages 4325–4334, 2017.

[26] Limin Wang, Yuanjun Xiong, Zhe Wang, Yu Qiao, Dahua Lin, Xiaoou Tang, and Luc Van Gool. Temporal segment networks for action recognition in videos. *PAMI*, 41(11):2740–2755, 2018.

[27] Yuetian Weng, Zizheng Pan, Mingfei Han, Xiaojun Chang, and Bohan Zhuang. An efficient spatio-temporal pyramid transformer for action detection. In *ECCV*, pages 358–375, 2022.

[28] Mengmeng Xu, Juan-Manuel Pérez-Rúa, Victor Escorcia, Brais Martinez, Xiatian Zhu, Li Zhang, Bernard Ghanem, and Tao Xiang. Boundary-sensitive pre-training for temporal localization in videos. In *ICCV*, pages 7220–7230, 2021.

[29] Mengmeng Xu, Chen Zhao, David S Rojas, Ali Thabet, and Bernard Ghanem. G-tad: Sub-graph localization for temporal action detection. In *CVPR*, pages 10156–10165, 2020.

[30] Chen-Lin Zhang, Jianxin Wu, and Yin Li. Actionformer: Localizing moments of actions with transformers. In *ECCV*, pages 492–510, 2022.

[31] Yue Zhao, Yuanjun Xiong, Limin Wang, Zhirong Wu, Xiaoou Tang, and Dahua Lin. Temporal action detection with structured segment networks. In *ICCV*, pages 2914–2923, 2017.

[32] Yue Zhao, Bowen Zhang, Zhirong Wu, Shuo Yang, Lei Zhou, Sijie Yan, Limin Wang, Yuanjun Xiong, D Lin, Y Qiao, et al. Cuhk & ethz & siat submission to activitynet

challenge 2017. *arXiv preprint arXiv:1710.08011*, 8(8), 2017.

[33] Zixin Zhu, Wei Tang, Le Wang, Nanning Zheng, and Gang Hua. Enriching local and global contexts for temporal action localization. In *ICCV*, pages 13516–13525, 2021.